unmodified and modified components. An approximate fit to this curve is then obtained by a proper choice of the parameters q and b in equation (9). When only unmodified scattering is being considered, the best fit is usually obtained with $q=0.0$, but when the interest is in both the unmodified and modified intensities, it is necessary to use a value of q other than zero. An exact fit is of course not to be expected, but if the departures are small and equally positive and negative, the errors are largely cancelled by the averaging which is involved. Suitable values of q and b having been determined, the values of $Q(2\theta,q,b)$ are obtained by interpolation from Table 1. With the use of equation (10), the ratio $I(2)/I(1)$ can be plotted over the desired range of 2θ.

As an illustration of the magnitude of second order scattering, we can take the example of vitreous SiO_2 with Rh $K\alpha$ radiation and an experimental technique which measures only the unmodified intensity (Warren & Mavel, 1965). From equation (8) we obtain for $I(2)/I(1)$ a value of about 0·08 in the range $2\theta=90°$ to $2\theta=180°$. Except for samples with high absorption coefficients, the second order scattering is in general large enough to require a correction.

This work was done in part at the Computation Center at the Massachusetts Institute of Technology, Cambridge. One of us (RLM) is a Raytheon Graduate Program Member at M.I.T.

References

WARREN, B. E. & MAVEL, G. (1965). *Rev. Sci. Instrum.* **36**, 196.

Acta Cryst. (1966). **21**, 461

Diffraction Contrast in Electron Microscopy of Chrysotile

BY E. J. W. WHITTAKER*

Ferodo Limited, Chapel-en-le-Frith, Stockport, England

(*Received* 24 *February* 1966)

Previous theoretical work on diffraction by chrysotile has not revealed the particular regions of the fibrils from which particular diffraction maxima originate. Difficulties in localizing these regions are overcome by a Fourier-transform method, and the results are applied to evaluating electron screening functions across the width of such fibrils on the basis of simple kinematical theory. The results show that under appropriate conditions electron micrographs of chrysotile fibrils may be expected to simulate hollow tubes even though the centres of the fibrils are filled either with amorphous material or with oriented ribbons of serpentine material.

Introduction

Electron microscopy provided the first evidence that chrysotile has a tubular structure (Turkevitch & Hillier, 1949; Bates, Sand & Mink, 1950). The evidence for this conclusion was based on the fact that electron microscope images of single chrysotile fibres frequently showed a central light band running along the length of the fibre with a darker band at each side. The boundaries between the light and dark bands are often remarkably sharp. This appearance has always been attributed to shielding of the electron beam by the fibre, this shielding being assumed to be a function of the material thickness traversed by the beam. Fig. 1, showing the variations in thickness across the section of a hollow cylinder, was used to demonstrate the theory by Noll & Kircher (1951). These workers extended the observations to stereoscopic electron micrographs of synthetic chrysotile, which gave a particularly convincing appearance of hollowness. Subsequent analysis of X-ray diffraction patterns of chrysotile showed these to be explicable in terms of cylindrically curved layers with a radius of the same order as that of the tubes deduced from electron microscopy, the layers being stacked together in numbers corresponding to the apparent wall-thicknesses of such tubes (Whittaker, 1953, 1956, 1957; Jagodzinski & Kunze, 1954; Jagodzinski, 1961). It has also been shown (Whittaker,

* Present address: Department of Geology & Mineralogy, Oxford, England.

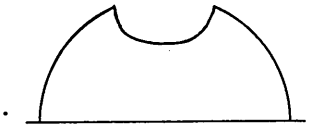

Fig. 1. The variation in material thickness across a section of a thick-walled hollow cylinder.

1963) that in high resolution electron diffraction it is possible to observe a fine structure within the diffraction maxima which corresponds to the expected interference between rays diffracted from the opposite walls of a tube with dimensions in accordance with the X-ray and electron microscope observations.

The fact which has been difficult to reconcile with the above observations is the density of chrysotile. This was shown by Pundsack (1956), and also by Kalousek & Muttart (1957), to be too high to admit the presence of the hollow tubes that had been postulated. More recent work by Pundsack (1961) and by Huggins & Shell (1965) has shown somewhat lower densities, which admit of a proportion of the postulated voids being present in some specimens, but nevertheless it appears likely that many chrysotile fibrils cannot be hollow. It has therefore been suggested (Whittaker, 1957) that the major part of the substance of chrysotile lies in tube walls as indicated by the diffraction evidence, but that the centres of these tubes are largely filled either by amorphous material or curved laths of the chrysotile structure. The appearance in the electron microscope then has to be explained either as a result of diffraction contrast between the walls and the infilling material, or as due to a tendency to select the less completely filled tubes in the preparation of specimens for electron microscopy. It is the purpose of the present paper to examine the possibility that diffraction contrast could arise, in a filled chrysotile tube, which would be of an appropriate kind and magnitude to explain the appearance in the electron microscope.

The polygonal approximation

The theoretical treatments of diffraction by cylindrical lattices which have been published hitherto (Jagodzinski & Kunze, 1954; Whittaker, 1954, 1955) have considered the total diffraction effects, but have not sought to identify particular regions of the lattice as giving rise to particular diffraction maxima. In order to evaluate diffraction contrast effects such an identification must be made.

The similarity of the diffraction pattern to a rotation photograph of a (suitably disordered) single crystal suggests that it should be possible to regard any particular diffraction maximum as arising from that part of the cylindrical lattice which has the same orientation as such a rotating crystal would have when it was producing a corresponding diffraction maximum. This is equivalent to the assumption that the cylindrical lattice may be approximated by a polygonal lattice, and that diffraction from any one side of such a polygonal lattice may be regarded as independent of that from the other sides. For simplicity, consider only the various orders of diffraction from the radial spacing, and suppose the polygon to be such that successive sides are in the appropriate Bragg positions to give rise to the successive orders from this spacing, as shown in Fig. 2. This approximation would appear to be a very artificial one, and would be expected to give a gross overestimate of the width (w) of the region of the lattice which is involved in the production of each diffraction maximum. It should therefore lead to an upper limit for w.

For the short wavelengths appropriate to electron diffraction we may put

$$\theta_h = h\lambda/2d$$

so that the angle between successive sides of the polygon is given by

$$\theta_{h+1} - \theta_h = \lambda/2d .$$

Hence

$$\begin{aligned} w &= 2R \sin \tfrac{1}{2}(\theta_{h+1} - \theta_h) \\ &= R\lambda/2d . \end{aligned}$$

Thus for a wavelength of 0·04 Å and a fibre diameter of about 300 Å, w is of the order of 0·4 Å. As this is a very small fraction of the lattice dimension, the concept of a reflexion from so narrow a strip of lattice plane is obviously meaningless, and is irreconcilable with the fact that the electron diffraction pattern is virtually identical with an X-ray diffraction pattern involving a value of λ (and therefore of w) about 40 times as big.

It must be concluded that the polygonal approximation is inadequate for the present purpose.

The Fourier transform approach

An alternative approach, to localize the regions of the circular lattice which give rise to particular diffraction maxima, is to divide the circular lattice into an arbitrary number of sectors, and to evaluate the contribution of each to the diffraction maximum. The choice of the number (and angular width) of the sectors will justify itself provided that the analysis shows the contributing region to include more than one sector.

In order to avoid complex amplitudes it is desirable to associate each sector of the circular lattice with its

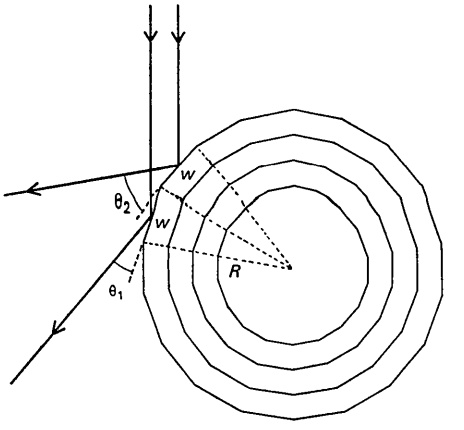

Fig. 2. Diffraction from a polygonal approximation to a cylindrical lattice. w is the maximum width of the region giving rise to a diffraction maximum if the two rays shown correspond to the 1st and 2nd orders of diffraction from the radial spacing.

centrosymmetrically related counterpart in a double sector as shown in Fig. 3(*a*). The Fourier transform of this is clearly the convolution of the transforms of the circular lattice [Fig. 3(*b*)] and the double sector aperture [Fig. 3(*c*)]. The general form of the transform of Fig. 3(*c*) was visualized by means of optical diffraction.

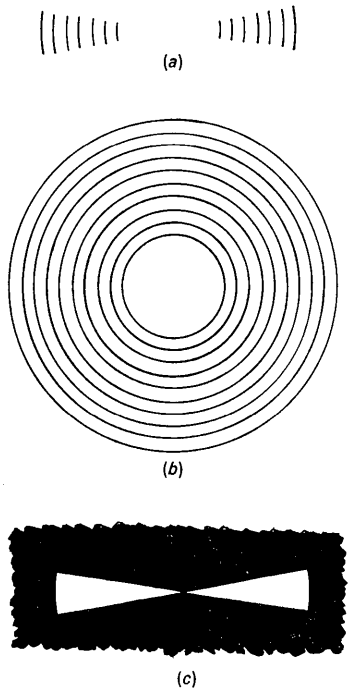

Fig. 3. (*a*) A double sector of the cross-section of a set of concentric circles. (*b*) The set of circles of which (*a*) forms a part. (*c*) A double sector aperture whose product with (*b*) gives (*a*). The Fourier transform of (*a*) is the convolution of the transform of (*b*) with that of (*c*).

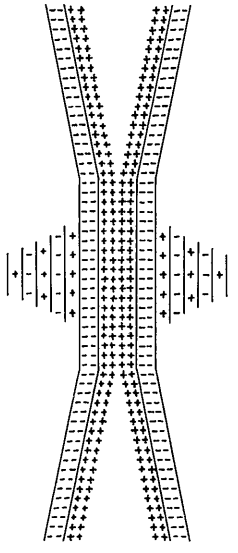

Fig. 4. Schematic representation of the appearance of the optical transform of Fig. 3(*c*). The lines correspond to loci of zero intensity, and the signs indicate the phases of the various fringes.

It consists principally of a double St. Andrew's cross with a straight portion at the intersection as shown schematically in Fig. 4, though there are also weak straight fringes at each side of the straight portion. For quantitative calculation the sectors were approximated by a pair of isosceles triangles, and central sections of the transform were calculated from the corresponding one-dimensional projections. These could always be resolved into sums and differences of triangular or trapezoidal functions which could be transformed by regarding them as convolutions of rectangular functions of appropriate breadths. Central sections of the transform were calculated at successive inclinations of 1° in the vicinity of the arms of the cross, but at much wider intervals remote from these directions where the sections cut the fringes much less obliquely. One quadrant of the transform of a double triangle with vertex angle 10° is shown as a contour map in Fig. 5.

The transform of the circular lattice of Fig. 3(*b*) is known from earlier work to consist of a set of concentric circles of radii h/a, where a is the radial spacing of the circles of Fig. 3(*b*). The convolution of the transforms of Fig. 3(*b*) and 3(*c*) therefore requires that we place the origin of Fig. 5 at all points on such a set of circles, while maintaining the orientation of the transform. Thus in order to evaluate the convolution at O (Fig. 6), with the circle of radius R, we must sum the contributions from transforms centred at all points such as O'. The contribution from the transform centred at O' is the value of this transform at O, *i.e.* at

$$x' = R(\cos\varphi - \cos\varphi') \quad y' = R(\sin\varphi - \sin\varphi')$$

where x', y' are the coordinates of O with respect to the rectangular axes of the transform at O', and φ, φ' are the position angles of O, O' shown in Fig. 6. Because of the centrosymmetry of the transform the value at x', y' of the transform centred at O' is equal to the value at O' of the transform centred at O, *i.e.* the value at

$$x = R(\cos\varphi' - \cos\varphi) \quad y = R(\sin\varphi' - \sin\varphi)$$

where x, y are the coordinates of O' with respect to the rectangular axes of the transform centred at O. Therefore the value of the convolution at any point such as O is equal to the integral of the transform centred at O along the circle with which it is to be convoluted.

In accordance with this result the convolution was performed by graphical integration, and hence it was found that the transform of Fig. 3(*a*) consists of a set of concentric circles of radii h/a on the first of which the weight varies with azimuth in such a way as to indicate that the contributions to the first order radial reflexions from different 10° sectors of a cylindrical lattice are as shown in Fig. 7.

From this result it may be concluded that, regardless of the sector angle used to analyse the situation, something like 90% of the amplitude of the first order of the reflexion from the 7·3 Å radial spacing originates within the three 10° sectors which most nearly lie in the 'Bragg orientation'. For higher order reflexions the

Fig. 5. Contour map of one quadrant of the calculated Fourier transform of a 10° double sector. Zero contours are broken and negative contours are dotted. The first one or two (positive or negative) contours are omitted in the most crowded regions.

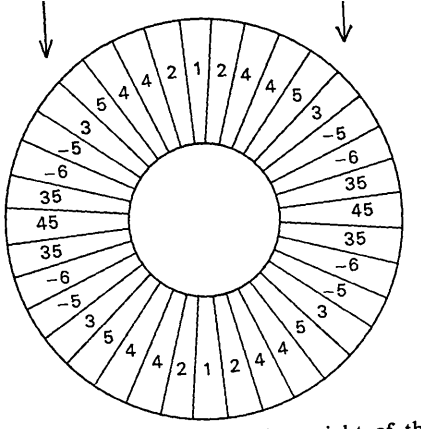

Fig. 7. Variation with azimuth of the weight of the Fourier transform of sectors like Fig. 3(*a*). In applying this result to the evaluation of shielding functions the incident radiation must be considered to be in the direction of the arrows.

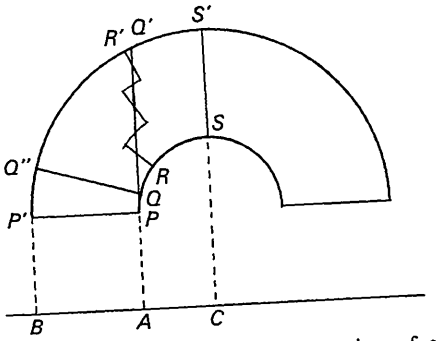

Fig. 8. The various regions of the cross-section of chrysotile fibre which contribute in different principal ways to the shielding function: $PP'Q''Q$ to the sharp reflexions, $QQ''Q'Q$ to the tails of the diffuse reflexions, and $SQQ'S'$ to the heads of the diffuse reflexions.

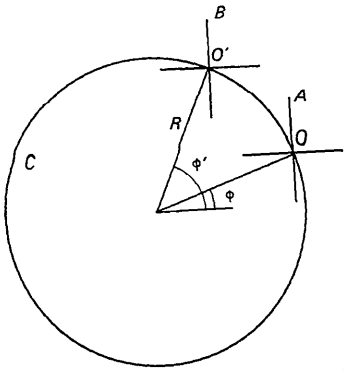

Fig 6. Diagram to illustrate the equivalence of the value at O [illegible] B and the circle C to the

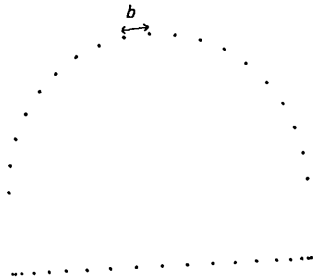

[illegible]

strongly contributing regions are even more concentrated; for the fifth order for example, 80% of the amplitude occurs within a single 10° sector.

Evaluation of the electron shielding function

It may be concluded that in the region AB of the projection of a quadrant of a fibril (Fig. 8) the electron image will be shielded from almost the whole of the energy which is diffracted into the sharp reflexions, and also from that part of the energy which is diffracted into the diffuse reflexions from outside the region $SQQ'S'$, which may for convenience be approximated by the stepped region $SRR'S'$. Conversely the region CA will be shielded only from the energy diffracted into diffuse reflections by $SRR'S'$.

The problem of locating the region from which a diffuse, cross-grating, reflexion arises is rather different from that for a sharp reflexion. In projection a cylindrically curved cross-grating has a variety of 'b-spacings' as shown in Fig. 9, and different regions may be considered to contribute to different parts of the tails of the reflexions according to the local value of the projection of the b-spacing. The slight delocalization of the regions of the structure contributing to different parts of the tail (corresponding to the analysis in the preceding section) may be neglected, since it will merely tend to make the electron shielding due to the diffuse reflexions more uniform than it would otherwise be. Thus if we divide up the 'tails' of the diffuse reflexions into the parts contributed by each 10° sector at various radii in the fibre, we shall tend to exaggerate the shielding in the region CA, relative to AB, since we shall assume that the more intense heads of the diffuse reflexions contribute only to the shielding in CA.

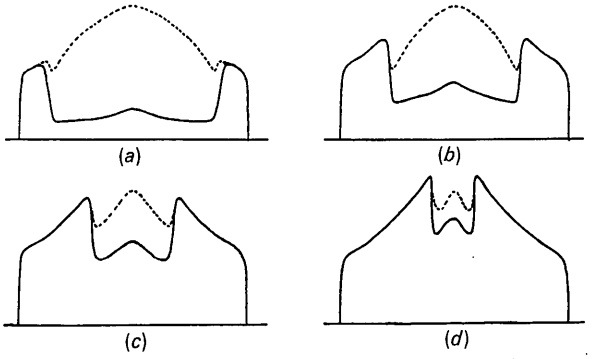

Fig. 10. The calculated shielding functions across the cross-sections of four fibrils with different ratios of internal to external radius: (*a*) 0·8, (*b*) 0·6, (*c*) 0·4 (*d*) 0·2. The full line is the shielding function for the empty cylinder. The broken line shows how this is modified if the tube is filled with amorphous material of the same density and composition as the walls.

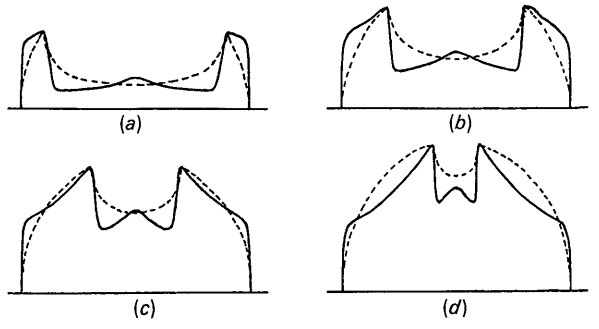

Fig. 11. Comparison of the shielding functions for empty tubes from Fig. 10 with the corresponding curves for material thickness penetrated by the beam (scaled to the same maxima).

The appropriate intensities and intensity distributions of the reflexions in electron diffraction were calculated approximately from the measured values in X-ray diffraction by use of a weighted mean ratio to allow for the different relationship to $\sin\theta/\lambda$ of the scattering factors in electron diffraction as compared with those in X-ray diffraction as follows:

$\sin\theta/\lambda$	Relative f_e/f_x
0–0·16	1·0
0·16–0·29	0·85
0·29–0·46	0·7
>0·46	0·5

Due allowance was also made for differences in the geometric factors. All the reflexions within the range of Cu $K\alpha$ radiation in X-ray diffraction were taken into account. Owing to the rapid fall-off of the scattering factor for electrons as a function of $\sin\theta/\lambda$ it seems likely that the effects of the generally weak higher order reflexions will be negligible. In fact 55% of the diffracted intensity is accounted for by the three strongest sharp reflexions together with the two strongest diffuse reflexions.

Shielding functions, giving relative values of electron intensity diffracted out of the direct beam as a function of position across a fibril, have been calculated for fibrils with a variety of ratios of internal diameter to external diameter, and are shown in Fig. 10.

When one has derived the shielding functions for empty tubes, it is a simple matter to derive corresponding functions for tubes which are filled with amorphous material of the same composition and density as the walls. Such material would necessarily have the same mean diffracting power as the material of the walls, and its effect on the shielding function would be proportional to the thickness of it to be penetrated. The broken lines show the effect of adding such shielding to the curves of Fig. 10.

Discussion

In Fig. 11 the shielding functions which have been calculated for hollow tubes are compared with the corresponding curves for thickness penetrated (scaled to the same maximum values). From this it may be seen that in every case the diffraction contrast theory will make an empty tube look 'emptier' than would

(*a*)

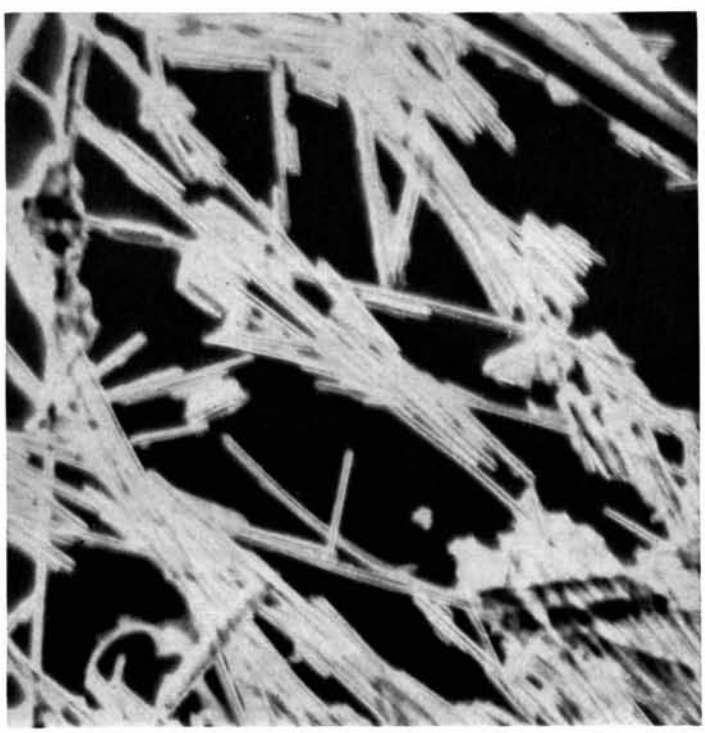

(*b*)

Fig. 12. Electron micrographs of the same chrysotile fibrils in (*a*) light field illumination, and (*b*) dark field illumination. (× 30,000).

[*To face p.* 466

the thickness contrast theory. This is especially true of the local contrast at the inner edge of the tube wall, which is of the greatest importance for visual perception of hollowness in a micrograph.

From Fig. 10(*d*) it may be seen that a solid fibril, in which there is a thick tubular wall based on a cylindrical lattice, and a thin amorphous core of the same density, would certainly be expected to appear empty. For rather thinner walls [Fig. 10(*c*) and (*b*)] the shielding in the centre would be greater than in the walls, but there would still be a contrast effect at the boundary of wall and core which would tend to give a visual appearance of 'emptiness'. Only when the wall is very thin [Fig. 10(*a*)] does this effect tend to disappear. Furthermore, amorphous material would in fact tend to be less dense than the ordered material in the wall; it would therefore diffract rather less than has been assumed, and this would enhance the appearance of emptiness.

No calculations have been made of the shielding function for tubes filled with oriented curved ribbons of chrysotile structure. But it is evident that these would diffract more than an amorphous filling if they were oriented with the layers approximately parallel to the beam so as to contribute to the sharp reflexions, but less than an amorphous filling if they were oriented so as not to contribute to the sharp reflexions. On a purely statistical basis the latter situation would occur the more frequently so that on this model one would expect a preponderance of fibrils which would appear more empty than would correspond to Fig. 10.

The relevance of diffraction contrast in the electron microscopy of chrysotile can be seen from a comparison of the dark field and light field electron micrographs in Fig. 12. Many fibrils which do not appear hollow in the light field photograph, as well as those which do, show contrast between the walls and the core on the dark field photograph.

The central maximum which occurs in all the curves of Fig. 10 would correspond to a dark median line within the light core. Such an effect is shown on a micrograph by Huggins & Shell (1965), and the effect is visible on some of the fibrils in Fig. 12(*a*).

It is evident that since the formation of diffraction contrast in an electron micrograph of chrysotile requires that the diffracted rays do not take part in the image formation, it will be diminished in circumstances which lead to resolution of the structural layers in the micrograph. It may therefore be significant that there is very little intensity contrast between walls and core in a micrograph of chrysotile (Dourmashkin, 1961) which just reveals fringes with a spacing of about 7 Å in the regions corresponding to *AB* in Fig. 8.

I wish to thank the Directors of Ferodo Limited for permission to publish this work; also Prof. H. Lipson for the use of his optical diffractometer to explore the optical transforms of sectors, Prof. C. A. Taylor for useful discussions of convolution methods, and Dr R. R. Dourmashkin for obtaining the dark field micrograph.

References

BATES, T. F., SAND, L. B. & MINK, J. F. (1950). *Science*, **111**, 512.
DOURMASHKIN, R. R. (1961). *Experimental Cell Research*, **25**, 480.
JAGODZINSKI, H. (1961). *Z. Elektrochem.* **65**, 313.
JAGODZINSKI, H. & KUNZE, G. (1954). *Neues Jb. Mineral Mh.* pp. 95, 113, 137.
KALOUSEK, G. L. & MUTTART, L. E. (1957). *Amer. Min.* **42**, 1.
NOLL, W. & KIRCHER, H. (1951). *Neues Jb. Min. Mh.* p. 219.
PUNDSACK, F. L. (1956). *J. Phys. Chem.* **60**, 361.
PUNDSACK, F. L. (1961). *J. Phys. Chem.* **65**, 30.
TURKEVITCH, J. & HILLIER, J. (1949). *Anal. Chem.* **21**, 475.
WHITTAKER, E. J. W. (1953). *Acta Cryst.* **6**, 747.
WHITTAKER, E. J. W. (1954). *Acta Cryst.* **7**, 827.
WHITTAKER, E. J. W. (1955). *Acta Cryst.* **8**, 261, 265, 726.
WHITTAKER, E. J. W. (1956). *Acta Cryst.* **9**, 855, 862, 865.
WHITTAKER, E. J. W. (1957). *Acta Cryst.* **10**, 149.
WHITTAKER, E. J. W. (1963). *Acta Cryst.* **16**, 486.